Available online at www.sciencedirect.com
ScienceDirect
Journal of Power Sources 159 (2006) 712–716
JOURNAL OF POWER SOURCES
www.elsevier.com/locate/jpowsour

Short communication

Electrochemical properties of a biodegradable polymer electrolyte applied to a rechargeable lithium battery

C. Polo Fonseca *, S. Neves

Laboratório Caracterização e Aplicação de Materiais (LCAM), Programa de Pós-Graduação Strictu Sensu em Engenharia e Ciência dos Materiais, Universidade São Francisco, 13251-900 Itatiba, SP, Brazil

Received 12 October 2005; received in revised form 27 October 2005; accepted 30 October 2005
Available online 27 December 2005

Abstract

A new solid polymer electrolyte, composed of a polymeric matrix of biodegradable polymer, poly-ε-caprolactone (PCL) and 10% $LiClO_4$ was used in a rechargeable lithium polymer battery. A $LiNiCoO_2$ film prepared by the combination of sol–gel synthesis and a template concept was used as the cathode. Cyclic voltammetry, charge/discharge cycle and electrochemical impedance spectroscopy, were used to characterize the Li|PCL, 10% $LiClO_4$|$LiNiCoO_2$ device. The specific charge/discharge capacity was determined to be 182 mAh g^{-1} in the first cycles and 120 mAh g^{-1} after 50 cycles. High lithium chemical diffusion coefficients values were obtained by electrochemical impedance spectroscopy.

Keywords: $LiNiCoO_2$; Polymer electrolyte; Batteries and biodegradation

1. Introduction

The use of electronic devices such as cell phones and laptop computers have been increasing, fostering the interest in research into their power-sources. The power-sources used in these devices are lithium batteries currently configured with a liquid electrolyte between the anode (lithium metal) and cathode (lithium metal oxide). The use of lithium metal offers the possibility of manufacturing highly specific energy batteries. However, rechargeable lithium metal batteries have a major problem related to the chemical surface products that develop on the lithium anode. Battery performance is closely related to the lithium surface and to the lithium/electrolyte interface properties (e.g., smooth lithium deposits, lack of dendrite formation upon cycling, reduced corrosion). Moreover, the use of a liquid electrolyte leads to problems, such as: leakage of a flammable electrolyte, production of gases upon overcharge or over discharge, as well as a thermal runaway reaction.

The use of solid-state devices can solve these problems. The solid polymer electrolyte rechargeable lithium batteries are expected to surpass the performance of conventional liquid electrolyte systems. The large-scale production of solid-state batteries could benefit from well-established technologies developed in the polymer industry. The key component of the lithium polymer battery is the electrolyte. The appropriate choice of this component is ruled by a series of requirements, which include high ionic conductivity, good mechanical properties and compatibility with the electrode materials.

P.V. Wright reported the first investigation on ionic conductivity of polymer electrolytes in 1973. In 1979, Armand et al. reported the first work on a polymeric electrolyte using the poly(ethylene oxide) (PEO) containing inorganic salt dissolved in its matrix and its possible application in lithium batteries. Polyethylene oxide (PEO) has demonstrated its good performance as a polymer solid electrolyte and many studies using PEO complexes with various lithium salts were reported. However, the high degree of crystallinity of PEO restricts its use in batteries. Attempts to improve the low ionic conductivity of this material have included the use of blends and copolymers of the PEO [1–4], gel electrolytes [5–9] and hybrid electrolytes [10–12]. Today's commercial lithium polymer technology is based on gel type polymer membranes in which an ion is immobilized in a solid polymer network, exhibiting semi-solid properties.

* Corresponding author. Tel.: +55 11 4534 8071; fax: +55 11 4524 1933.
E-mail address: carla.fonseca@saofrancisco.edu.br (C. Polo Fonseca).

0378-7753/$ – see front matter © 2005 Elsevier B.V. All rights reserved.
doi:10.1016/j.jpowsour.2005.10.095

In a previous report [13], we described a new polymeric electrolyte based on a biodegradable polymer, poly-ε-caprolactone (PCL) as the polymeric matrix with lithium salt. The use of biodegradable polymers has contributed to a reduction in environmental problems. As a result, there has been a trend towards the production of degradable natural and synthetic polymers and natural/synthetic polymer blends. Among biodegradable synthetic polymers, PCL is one of the most attractive due to its availability; it can degrade in an aqueous medium or in contact with microorganisms, and has good mechanical properties. In previous work the possibility of producing a biodegradable polymer electrolyte based on poly-ε-caprolactone (PCL) with $LiClO_4$ was investigated. The maximum ionic conductivity obtained at room temperature was 1.2×10^{-6} S cm^{-1} for PCL complexes with 10 wt.% $LiClO_4$. In this mixture, complete biodegradation occurred after 110 days. The large electrochemical stability window of approximately 5 V showed that the PCL/$LiClO_4$ electrolyte has important electrochemical properties that would make it useful in the production of rechargeable batteries with a lower environmental impact.

The purpose of this work is to apply a biodegradable solid polymer electrolyte to a lithium battery with the goal of preventing or reducing dendrite formation, leakage electrolyte, and more importantly for low environmental impact when the device is discarded. The electrochemical properties of the interface electrode/electrolyte and electrochemical stability were evaluated.

2. Experimental details

2.1. Solid biodegradable polymer electrolyte preparation

The biodegradable electrolyte solution was prepared by dissolving PCL (Union Chemical Carbide Ltd. (P-767) and a weight average molecular weight (M_w) of 80,000) and 10.0% $LiClO_4$ in tetrahydrofuran (THF). The solvent was evaporated and dried at high vacuum for 72 h.

2.2. $LiNiCoO_2$ synthesis

The metal complex precursor was prepared by mixing $Co(CH_3COO)_2{\cdot}2H_2O$, $Ni(CH_3COO)_2$ and $LiCH_3COO{\cdot}4H_2O$ (Aldrich) in a Li:Co:Ni atomic ratio of 1:1:1 in citric acid and ethylene glycol (1:3) solution. Citric acid as a chelating agent was used for the slurry to provide a homogeneous distribution and prevent precipitation of the cathode material. The sol–gel precursor obtained had a pink coloration. To obtain the annealing temperature of the gel precursor a differential thermal analysis (DTA) of the sol–gel precursor was done.

Porous $LiNiCoO_2$ film was synthesized combining the concepts of sol–gel and template synthesis for which the host membrane was previously prepared [20].

2.2.1. Membrane preparation

A 10 wt.% solution of cellulose acetate (CA) (Aldrich M_w = 50,000) in acetic acid was spin-coated onto ITO glass (5000 rpm during, 5 s). Phase separation was achieved by immediate immersion in water for 30 s.

2.2.2. Film preparation

After drying the membrane in atmosphere it was immersed into the sol–gel precursor. The films were annealed using the following temperature routine: (i) from room temperature to 250 °C at 1 °C min^{-1}; (ii) at 250 °C for 15 min; (iii) from 250 to 550 °C at 5 °C min^{-1} and (iv) at 550 °C for 15 min. After annealing, homogeneous films with a brown coloration were obtained. The film thickness was determined to be 2.23 μm by an alpha step profilometter.

2.3. Li|PCL, 10% $LiClO_4$|$LiNiCoO_2$ device

The electrochemical cell consisted of two electrodes with a lithium foil pressed onto copper plate current collectors as the reference and counter electrode, ITO plate covered with mixed oxide was the working electrode. Electrochemical data were obtained using 10% $LiClO_4$ in poly(ε-caprolactone) (PCL) as the polymeric electrolyte. One hundred microliters of electrolyte solution was dropped onto the cathode. The electrode/electrolyte was dried for 72 h in vacuum and enclosed with lithium foil in an argon-filled dry box. The cell consisted of: Li|PCL, 10% $LiClO_4$|$LiNiCoO_2$.

All the electrochemical experiments were done into a dry box. The electrochemical cells were characterized using cyclic voltammetry, in the potential range from 2.5 to 4.3 V at 5 mVs^{-1}, and by charge/discharge cycle with a current density of ±10 μA cm^{-2}. For electrochemical impedance spectroscopy, an ac amplitude of 10 mV was applied to the Li|PCL, 10% $LiClO_4$|$LiNiCoO_2$ system and data were collected in the frequency range 10^5 to 10^{-2} Hz. All electrochemical experiments were performed using an AUTOLAB-PGSTAT30 FRA.

3. Results and discussion

3.1. Biopolymeric solid polymer electrolyte

PCL/$LiClO_4$ films show good mechanical properties [14] and with slight coloration. Pure PCL is a semi crystalline material with 30% crystallinity, with T_m = 56.0 °C and T_g = −47 °C [13].

3.2. Morphologic analysis of the $LiNiCoO_2$ cathode

The porous $LiNiCoO_2$ film was synthesized by the combination of the concepts of sol–gel synthesis and template preparation. This combination of methods was utilized by other authors [15,16], however, the main difference in this work is the host membrane utilized, which was produced using a phase inversion technique. This membrane was used as a "mold" for some types of synthesis such as conducting polymers and transition metal oxide materials [17,18].

The $LiNiCoO_2$ film was produced by loading the host membrane with the sol–gel precursor following by annealing. A temperature increase was promoted by the coalescence of the

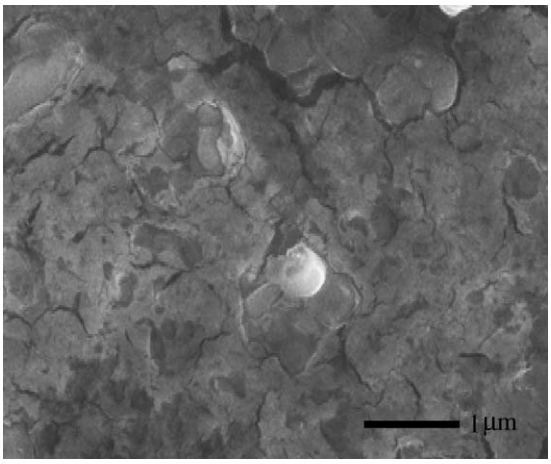

Fig. 1. Scanning electron micrograph of the $LiNiCoO_2$ film.

nanoparticle oxide into the porous membrane. Spherical particles grew together on membrane cracking. In the final annealing step, the host matrix was completely eliminated and the oxide was produced. The porous film morphologies exhibited fine monodispersed spherical particles coalescence with a cracked surface (Fig. 1).

In previous work we showed that these pores promoted improvement in the ionic transport at the electrode/electrolyte interface [17,19,20].

3.3. Li|PCL, 10% $LiClO_4$|$LiNiCoO_2$ device characterization

The intercalation/de-intercalation lithium ion process in the Li|PCL, 10% $LiClO_4$|$LiNiCoO_2$ device was analyzed by cyclic voltammetry with a scan rate of 5.0 mV s^{-1}, Fig. 2. The curve shows an anodic peak at 4.02 V and two-cathodic peaks for the first cycle. After five redox cycles the system was stable with a 93% coulombic efficiency. Two anodic peaks at 3.77 and 3.97 V and two cathodic peaks at 3.8 and 3.22 V were observed after the stabilization of the system. The presence of the two peaks in the cyclic voltammetry is evidence of the presence of two types of crystallographic sites for the insertion/extraction of the lithium

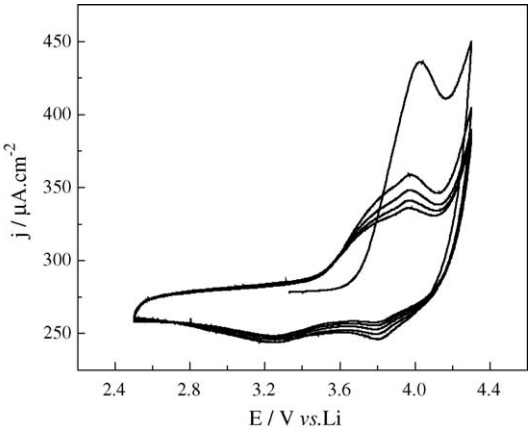

Fig. 2. Cyclic voltammograms of Li|PCL, 10% $LiClO_4$|$LiNiCoO_2$ at 5 mV s^{-1}.

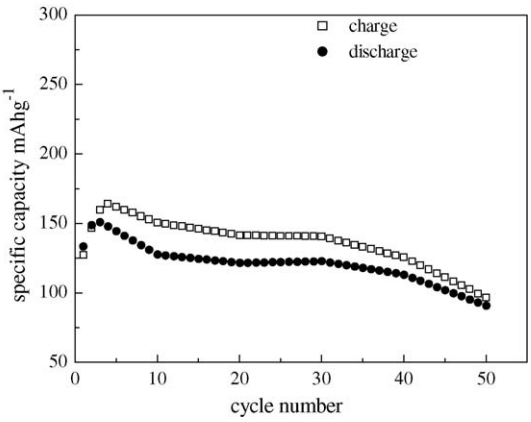

Fig. 3. Charge and discharge curves of the Li|PCL, 10% $LiClO_4$|$LiNiCoO_2$ system, $j = \pm 10\ \mu A\ cm^{-2}$.

ions. This fact is due to the presence of Ni in the oxide film composition changing the spinal structure of the $LiCoO_2$. The distance between the anodic and cathodic peaks is only 0.19 V indicating a low resistance at the electrode/electrolyte interface.

Fig. 3 shows the specific capacity of the charge/discharge curves as a function of cycle number. The curve showed a low hysteresis for the intercalation/de-intercalation lithium ion process. The charge/discharge specific capacity for the Li|PCL, 10% $LiClO_4$|$LiNiCoO_2$ system exhibited a similar value to the literature, 182 mAh g^{-1} in the first cycle and 120 mAh g^{-1} after 50 cycles [21,24]. In the first charge/discharge cycle an increase in the specific capacity was observed. This fact was attributed to the accommodation of the electrolyte/electrode interface. After this accommodation process the curve shows a gradual decline.

This decrease of the charge/discharge specific capacity with the increase of the number of cycles was evaluated by electrochemical impedance spectroscopy. A Nyquist plot of Li|PCL, 10% $LiClO_4$|$LiNiCoO_2$ initially and after 50 cycles at the open circuit voltage ($E = 3.15$ V) is presented at Fig. 4. The EIS measurements were done monitoring the dc current response to ensure that the system reached an equilibrium after cycling at

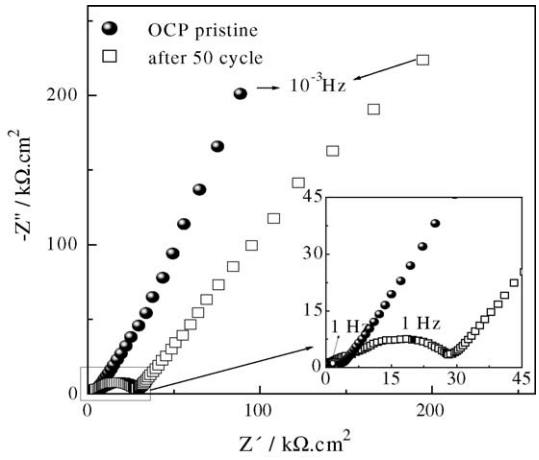

Fig. 4. Nyquist diagram at the OCV potential (3.15 V) and after 50 cycles. Perturbation amplitude 10 mV.

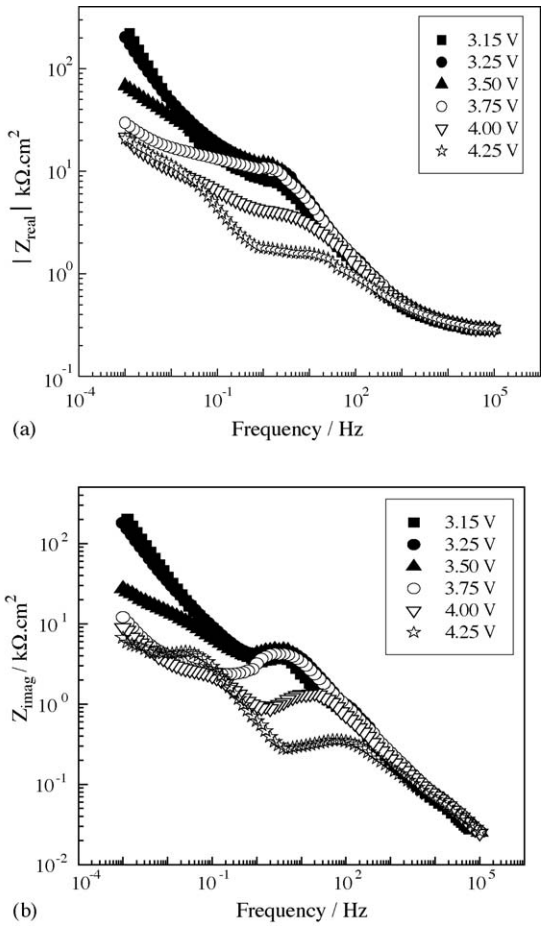

Fig. 5. Frequency dependence of the impedance of real (a) and imaginary (b) parts of the Li|PCL, 10% $LiClO_4$|$LiNiCoO_2$ system.

open circuit. A depressed semicircle is seen at high-medium frequency in the impedance spectrum. The presence of a semicircle at this frequency range is due to the charge transfer resistance (R_{ct}) during the intercalation/de-intercalation lithium ion process that occurs in the electrode/electrolyte interface region. Upon continuous charge/discharge cycles, the diameter semicircle increases indicating an increase of the R_{ct} value (Fig. 4). This behavior is related to the surface film formation on the cathode [22–25] leading to a charge/discharge specific capacity decline.

At intermediate and lower frequencies an inclined line suggests a lithium ion diffusion behavior. Although, the ionic conductivity of the biodegradable polymer electrolyte is lower than for a liquid electrolyte, the ion diffusion phenomena could be explained by a homogenous distribution of the biodegradable polymer electrolyte in the pores of the cathode, which makes the diffusion path of ion species shorter.

Electrochemical behavior as a function potential applied was analyzed by electrochemical impedance spectroscopy after system stabilization. The electrochemical characteristics are clearer if we plot the EIS data in a Bode type as shown in Fig. 5a and b. Fig. 5a shows the Bode plot of real part of the EIS ($|Z_{Re}|$). The electrochemical impedance spectroscopy (EIS) measurements were done at fixed potential from OCV to 4.25 V at 250 mV

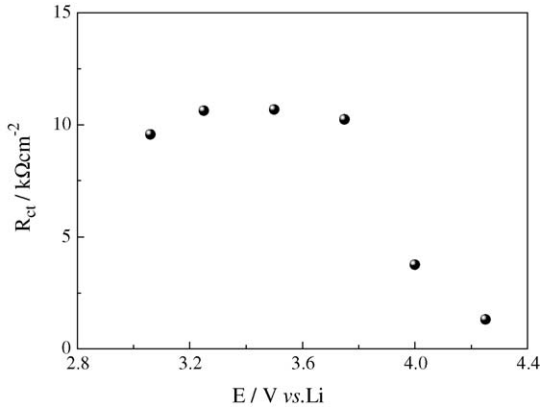

Fig. 6. Variation in the charge transfer resistance (R_{ct}) as a function of the potential applied.

intervals. At each potential, the dc current response was monitored to ensure that the electrode reached equilibrium at a given potential prior to the EIS measurements. The electrolyte resistance ($R_e \approx 300\,\Omega\,cm^2$) was obtained through an impedance value of the plateau observe at high frequency. Another plateau was observed at intermediate frequency.

The difference between the plateaus observed at low and intermediate frequency corresponds to the charge-transfer resistance attributed to lithium de-intercalation process of the $LiNiCoO_2$. The dependence of the charge-transfer resistance on the applied potential is show in Fig. 6. R_{ct} decreased started after the 3.75 V, in agreement with the de-intercalation process seen in the cyclic voltammetry (Fig. 2). This charge-transfer resistance decrease indicates an increase of the $LiNiCoO_2$ conductivity with the lithium ions extraction process. Similar behavior was also seen in the Bode plots of the imaginary parts of the EIS (Z_{imag}) in Fig. 5b.

The chemical diffusion coefficient as a function of the potential applied is shown in Fig. 7. The chemical diffusion coefficient was obtained in accordance with Ho et al. [26]. The large chemical diffusion coefficient values observed for the Li|PCL, 10% $LiClO_4$|$LiNiCoO_2$ system can be attributed to the nature of the morphology of the surface electrode that has a high surface area due to the porous nature originating from cracks in the surface.

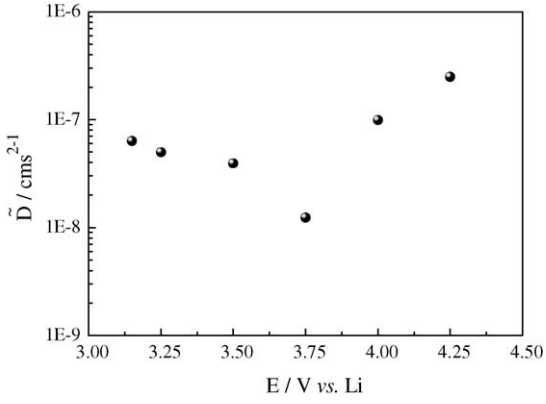

Fig. 7. Variation in the chemical diffusion coefficient as a function of the potential applied.

The ionic conductivity increased due to the impregnated polymer electrolyte. Inside the porous electrode body, the dispersed particles may act as single electrodes with nm sizes, nevertheless the chemical diffusion coefficient values are determined by the overall thickness of the electrode. This may cause a significant increase in the chemical diffusion coefficient values.

4. Conclusion

In this work we present the potential application of a new solid biodegradable polymeric electrolyte in a lithium battery. The solid biodegradable polymer electrolyte was a polymeric matrix of the biodegradable polymer, poly-ε-caprolactone (PCL) and 10% $LiClO_4$. The $LiNiCoO_2$ cathode films were produced by the combination of the concepts of sol–gel synthesis and template.

Although the ionic conductivity of the solid biodegradable polymer electrolyte is relatively low, the synergistic combination of the oxide film and the electrolyte promoted high values of ionic diffusion resulting in appreciable specific capacity values. Some modifications such as addition of a plasticizing agent and substitution of $LiClO_4$ by a safer salt, may be more practical. The work continues on these modifications.

Acknowledgements

This work was supported by FAPESP (grant 03/02662-09), CNPq (grants 477942/2003-2 and 303500/2002-6) and Universidade São Francisco.

References

[1] K. Nagaoka, H. Nasure, I. Shinohara, J. Polym. Sci. Polym. Lett. 22 (1984) 659.
[2] R.A. Zoppi, C. Polo Fonseca, M.-A. De Paoli, S.P. Nunes, Solid State Ionics 91 (1996) 123.
[3] A. Bakker, J. Lindgren, K. Hermansson, Polymer 37 (1996) 1871.
[4] C.N.P. Fonseca, T.T. Cezare, S. Neves, J. Power Sources 112 (2002) 395.
[5] Z. Florjanczyk, W. Bzducha, N. Langwald, J.R. Dygas, F. Krok, B. Misztal-Faraj, Electrochim. Acta 45 (2000) 3563.
[6] B.B. Owens, P.M. Skarstad, D.F. Untereker, Solid-electrolytes cells, in: D. Linden (Ed.), Handbook of Batteries, 2nd ed., McGrraw-Hill Book, New York, 1995 (Chapter 15).
[7] H. Akashi, K. Sekai, K.-I. Tanaka, Electrochim. Acta 43 (1998) 1193.
[8] G.G. Kumar, N. Munichandraiah, Electrochim. Acta 44 (1999) 2663.
[9] C.N.P. Fonseca, S. Neves, J. Power Sources 104 (2002) 85.
[10] R.A. Zoppi, C. Polo Fonseca, M.-A. De Paoli, S.P. Nunes, Acta Polym. 48 (1997) 131.
[11] D.A. Loy, K.J. Shea, Chem. Rev. 95 (1995) 1431.
[12] U. Schubert, N. Husing, A. Lorenz, Chem. Mater. 7 (1995) 2010.
[13] C. Polo Fonseca, D.S. Rosa, F. Gaboardi, S. Neves, J. Power Sources, in press.
[14] D.S. Rosa, I. Chiavatto Neto, M.R. Calil, A.G. Pedroso, C.P. Fonseca, S. Neves, J. Appl. Polym. Sci. 91 (2004) 3909.
[15] B.B. Lakshmi, C.J. Patrissi, C.R. Martin, Chem. Mater. 9 (1997) 2544.
[16] M.A. Aegerter, R.C. Mehrota, I. Oehme, R. Reisfeld, S. Sakka, O. Wolfbers, C.K. Jorgensen, Optical and Electronic Phenomena in Sol–Gel Glasses and Modern Applications Structure and Banding, vol. 85, Springer-Verlag, Berlin, 1996.
[17] S. Neves, R.F. Santos, W.A. Gazotti, C. Polo Fonseca, Thin Solid Films 460 (2004) 294.
[18] S. Neves, C. Polo Fonseca, J. Braz. Chem. Soc. 15 (2004) 395.
[19] C. Polo Fonseca, M.C.A. Fantini, S. Neves, Thin Solid Films 488 (2005) 68.
[20] C. Polo Fonseca, S. Neves, J. Power Sources 135 (2004) 249.
[21] G. Ting-Kuo Fey, R.F. Shiu, T. Prem Kumar, C.L. Chen, Mater. Sci. Eng. A 100 (2003) 234.
[22] D.P. Abraham, R.D. Twesten, M. Balasubramanian, I. Petrov, J. McBreen, K. Amine, Electrochem. Commun. 4 (2002) 620.
[23] D. Ostovsky, F. Ronci, B. Scrosati, P. Jacobson, J. Power Sources 94 (2001) 183.
[24] C.H. Chen, J. Liu, K. Amine, Electrochem. Commun. 3 (2001) 44.
[25] C.H. Chen, J. Liu, M.E. Stoll, G. Henriksen, D.R. Vissers, K. Amine, J. Power Sources 128 (2004) 278.
[26] C. Ho, I.D. Raistrick, R.A. Huggins, J. Electrochem. Soc. 127 (1980) 343.